

1 **Supplementary information for:**
2 **Bare soil albedo at high spatial and temporal resolution from**
3 **Sentinel-2 observations over Europe**
4

5 Ke Yu¹, Yang Su^{1,2,3,*}, Philippe Ciais¹, Ronny Lauerwald^{2,4}, David Makowski⁵, Tianqi Shi¹,
6 Shengbiao Wu⁶, Petra Sieber⁷, Chuanlong Zhou¹, Daniel S. Goll¹

7 ¹Laboratoire des Sciences du Climat et de l'Environnement, LSCE/IPSL, CEA-CNRS-UVSQ,
8 Université Paris-Saclay, 91191 Gif-sur-Yvette, France.

9 ²UMR ECOSYS, INRAE AgroParisTech, Université Paris-Saclay, 91120 Palaiseau, France

10 ³Département d'Informatique, École Normale Supérieure - PSL, 75005 Paris, France

11 ⁴Department Geoscience, Environment & Society-BGEOSYS, Université Libre de Bruxelles,
12 Bruxelles, Belgium

13 ⁵UMR MIA PS, INRAE AgroParisTech, Université Paris-Saclay, 91120 Palaiseau, France

14 ⁶Future Urbanity & Sustainable Environment (FUSE) Lab, Division of Landscape Architecture,
15 Department of Architecture, Faculty of Architecture, The University of Hong Kong, Pokfulam,
16 Hong Kong Special Administrative Region, China

17 ⁷Institute for Atmospheric and Climate Science, ETH Zurich, Zurich, Switzerland

18
19
20

21 **Table of contents**

22

23 Supplementary Text 3

24 Supplementary Text 1.1 The 10-fold cross-validation in the random forest model..... 3

25 Supplementary Figures 4

26 Supplementary Figure 1 4

27 Supplementary Figure 2 5

28 Supplementary Figure 3 6

29 Supplementary Figure 4 7

30 Supplementary Figure 5 8

31 Supplementary Figure 6 9

32 Supplementary Figure 7 10

33 Supplementary Figure 8 11

34 Supplementary Figure 9 12

35 References..... 13

36

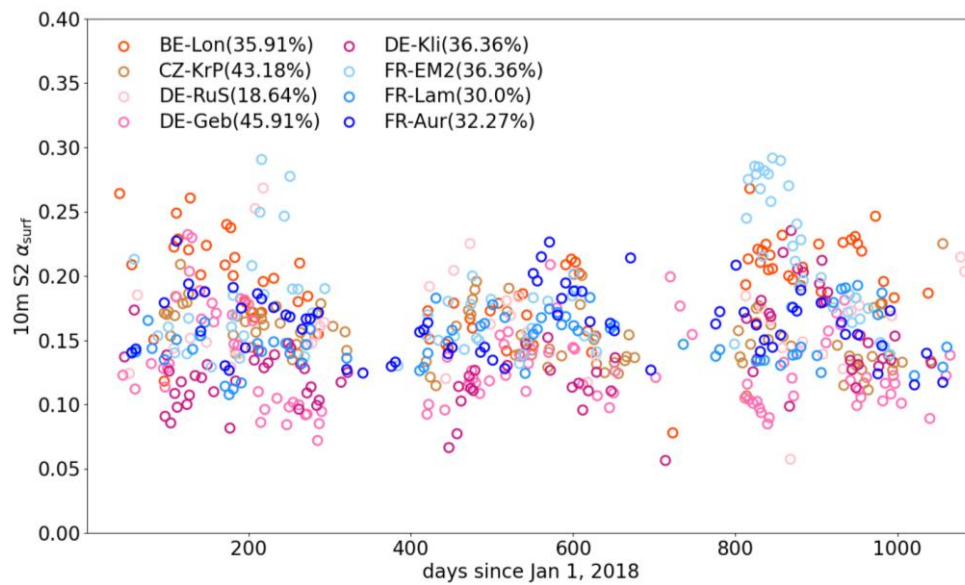
37

38 **Supplementary Text**

39 **Supplementary Text 1.1 The 10-fold cross-validation in the random** 40 **forest model**

41 The 10-fold cross-validation divided the training dataset into 10 subsets: 90% for the training
42 model with specified hyperparameters and 10% for validation in each subset. The trained model
43 then predicted the dependent variable using selected features in the 10% validation dataset, and
44 both the dependent variable and the selected features were recorded. During the process, the
45 importance of each feature is calculated based on how much each feature contributes to
46 decreasing the impurity (measured by Gini index) in the tree nodes across all the trees in the
47 forest. Higher scores indicate more important predictors (Strobl et al., 2008). After processing
48 all 10 subsets, the overall hyperparameter-specific coefficient of determination (R^2) and root
49 mean square error (RMSE) were calculated based on the aggregated dependent variable and the
50 selected features from all subsets. The above procedure was repeated for all pairs of
51 hyperparameters and the ones with the highest R^2 were selected to define the final random forest
52 model. Note that the RMSE values for all hyperparameter pairs remain consistently around 0.02.

53 **Supplementary Figures**



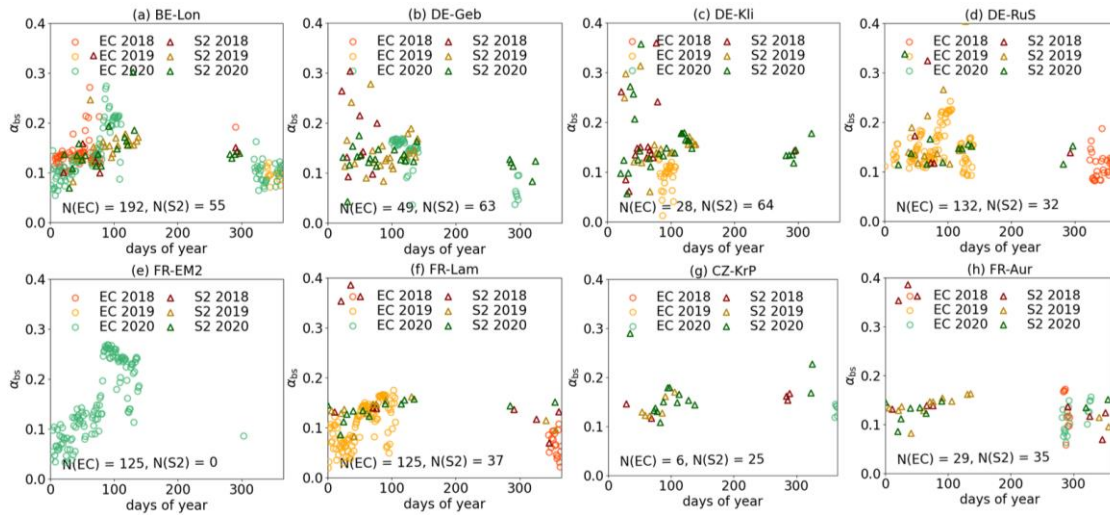
54

55 **Supplementary Figure 1** The dynamics of 10m 5-day Sentinel-2 surface albedo at 8 ICOS
56 sites from 2018 to 2020. The numbers in legend brackets represent the percentage of available
57 data (%) in three years.

58

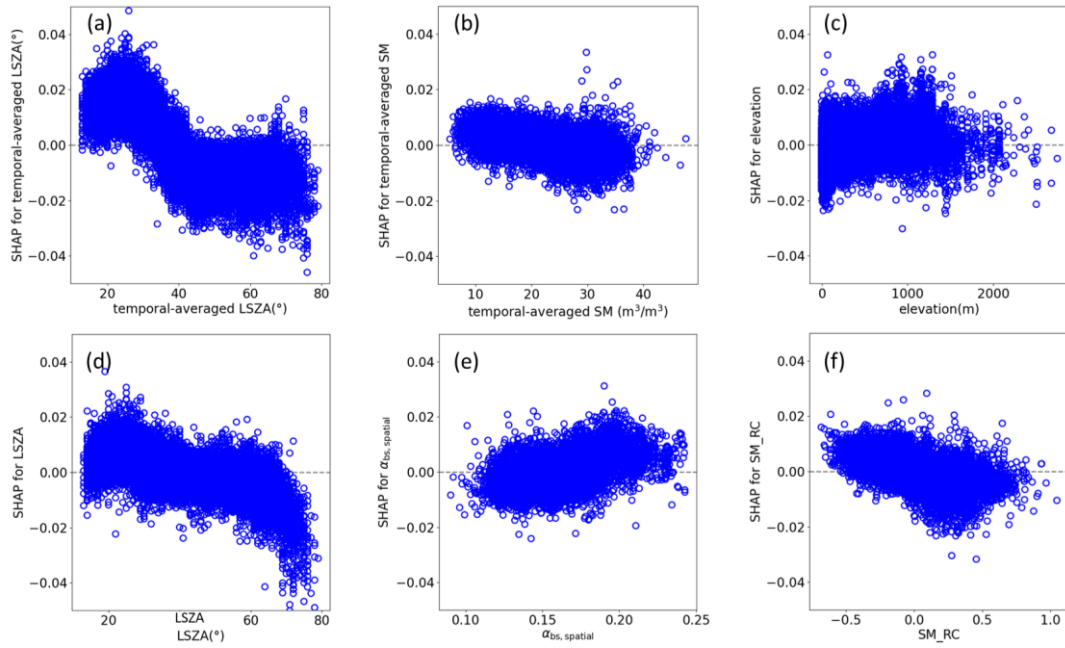
59

60



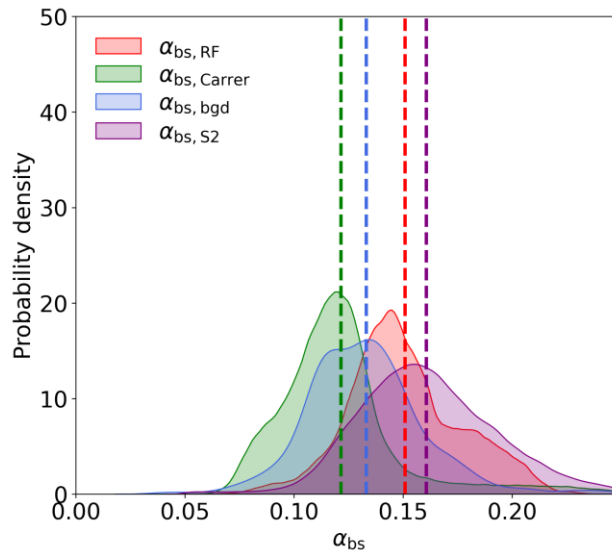
61

62 **Supplementary Figure 2** The bare soil albedo extracted from Sentinel-2 (S2) surface albedo
63 product ($\alpha_{bs, S2}$, triangles) and computed by site eddy covariance (EC) measurements ($\alpha_{bs, site}$,
64 circles) during the same bare soil periods detected by field photos instead of satellite vegetation
65 indices at 8 ICOS sites from 2018 to 2020 (Table 3). ‘EC’ and ‘S2’ in each plot mean eddy
66 covariance and Sentinel-2, respectively. ‘N’ is the number of dots



67

68 **Supplementary Figure 3** The Shapley Additive exPlanations (SHAP) Values of the top 3
 69 selected features in the spatial random forest model ((a)-(c)), and in the temporal random forest
 70 model ((d)-(f)). ‘LSZA’, ‘SM’ and ‘SM_RC’ represent the local solar zenith angle, soil
 71 moisture and relative SM anomaly, respectively. $\alpha_{bs, spatial}$ is the spatial bare soil albedo
 72 distribution predicted by the spatial random forest model. The blue dots represent the
 73 contribution of each feature to bare soil albedo variation.

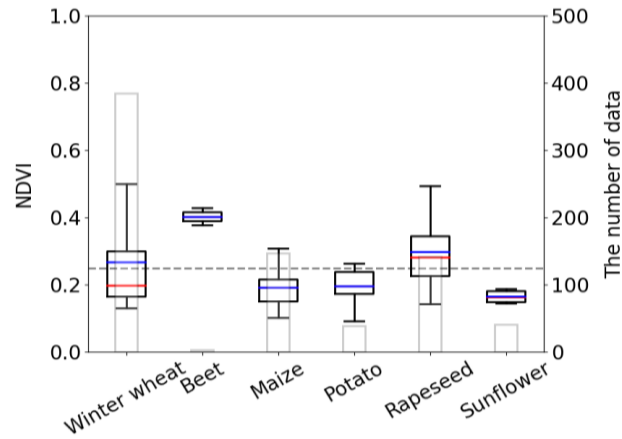


74

75 **Supplementary Figure 4** The probability density of different bare soil albedo (α_{bs}) products
 76 within the European cropland regions. The $\alpha_{bs, RF}$ is produced by the trained random forest
 77 models from 2018 to 2020, with 300 m spatial resolution and 5-day intervals. $\alpha_{bs, Carrer}$ and $\alpha_{bs,}$
 78 bgd are derived from 8-day 1 km α_{bs} map (Carrer et al., 2014) and a monthly 50 km α_{bs} map
 79 (Pinty et al., 2011), respectively. $\alpha_{bs, S2}$ is the α_{bs} datasets trained in random forest models
 80 obtained from Sentinel-2 surface albedo observation (Lin et al., 2023) using vegetation indices
 81 (see Methods).

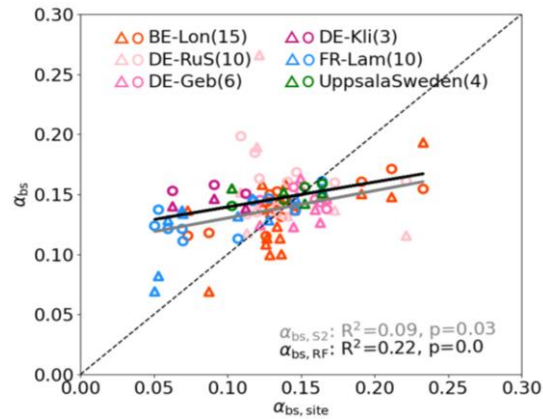
82

83



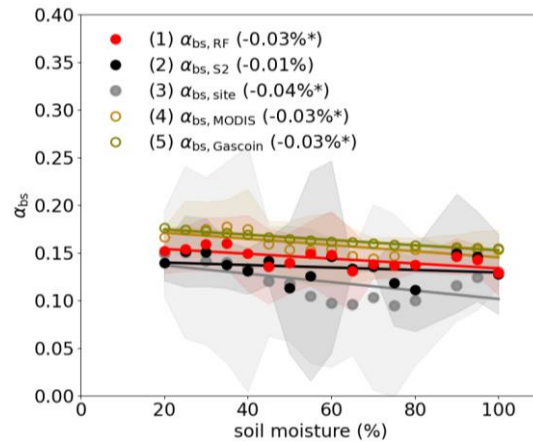
84

85 **Supplementary Figure 5** The NDVI distribution of crop residues at 6 European cropland sites
86 from 2018 to 2020. The NDVI datasets were derived from 5-day Sentinel-2 reflectance product
87 with a spatial resolution of 300 m on the Google Earth engine platform. The residue periods
88 were identified by daily or weekly site photos. The red and blue lines in each figure represent
89 the median and mean NDVI, respectively. The gray line represents the NDVI threshold of 0.25
90 used to extract bare soil periods and the corresponding Sentinel-2 bare soil albedo samples.



92

93 **Supplementary Figure 6** The linear relationship between $\alpha_{bs, RF}$ and $\alpha_{bs, site}$ (circles, black line),
 94 and between $\alpha_{bs, S2}$ and $\alpha_{bs, site}$ (triangles, gray line) at 4 sites during the same bare soil periods
 95 from 2018 to 2020. The bare soil periods are detected by field photos instead of satellite
 96 vegetation indices. The $\alpha_{bs, RF}$ is produced by the trained random forest models. The $\alpha_{bs, S2}$
 97 is extracted from the Sentinel-2 surface albedo products, while $\alpha_{bs, site}$ is computed by site eddy
 98 covariance measurements (Table 3). Different colors represent different sites. The gray and
 99 black lines are the fitting trends between $\alpha_{bs, site}$ and $\alpha_{bs, S2}$, and between $\alpha_{bs, site}$ and $\alpha_{bs, RF}$,
 100 respectively. The numbers in the legend brackets represent the sample size. The black dotted
 101 line is 1:1 line. R^2 and p are the coefficient of determination and significance level.

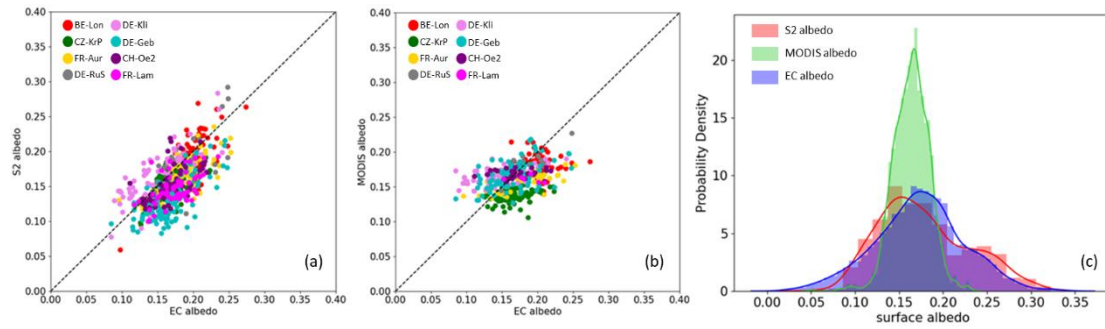


102

103 **Supplementary Figure 7** The linear relationship between $\alpha_{bs, \text{site}}$ and soil moisture (SM), $\alpha_{bs, \text{RF}}$
 104 and SM, $\alpha_{bs, \text{MODIS}}$ and SM, and $\alpha_{bs, \text{Gascoin}}$ and SM, respectively (see Table 3). The superficial
 105 SM dataset in the x-axis is derived from daily soil sensor measurements which have an SM step
 106 of 5% during the same bare soil periods from 2018 to 2020. The dots with areas in different
 107 colors show the averages and 2-time standard deviations of all datasets in each SM step. The
 108 $\alpha_{bs, \text{RF}}$ is produced by the trained random forest models using daily GSSM SM product as one
 109 of the predictors (red dots). The $\alpha_{bs, \text{S2}}$ is extracted from the Sentinel-2 surface albedo products
 110 (black dots), while $\alpha_{bs, \text{site}}$ is computed by site eddy covariance measurements (gray dots). The
 111 $\alpha_{bs, \text{MODIS}}$ is extracted from 500m daily MODIS surface albedo product (MCD43A3) (yellow
 112 hollow dots). $\alpha_{bs, \text{Gascoin}}$ is computed by the function of SM using the 1km GSSM SM product
 113 (brown dots). ‘*’ means the linear relationship (solid lines) passes the significance level of 0.05.

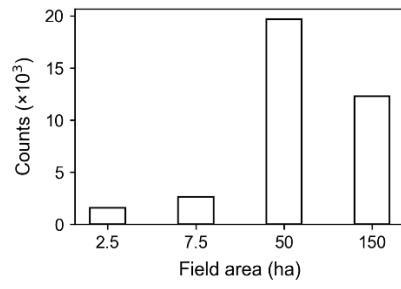
114

115



116

117 **Supplementary Figure 8** The comparison of surface albedo at 8 cropland sites during the same
118 periods between (a) Sentinel-2 (300m, 5-day) and site measurements; (b) MODIS surface
119 albedo product (500m, daily) and site measurements. (c) represent the probability density of the
120 surface albedo from Sentinel-2 data, MODIS product and site measurements.



121

122 **Supplementary Figure 9** The count of field sizes of LUCAS 2018 farms.

123 **References**

124

125 Carrer, D., Meurey, C., Ceamanos, X., Roujean, J. L., Calvet, J. C., and Liu, S. L.: Dynamic mapping
126 of snow-free vegetation and bare soil albedos at global 1 km scale from 10-year analysis of MODIS
127 satellite products, *Remote Sens. Environ.*, 140, 420-432, doi: 10.1016/j.rse.2013.09.005, 2014.

128

129 Lin, X., Wu, S., Chen, B., Lin, Z., Yan, Z., Chen, X., Yin, G., You, D., Wen, J., Liu, Q., Xiao, Q.,
130 Liu, Q., and Laforzezza, R.: Estimating 10-m land surface albedo from Sentinel-2 satellite
131 observations using a direct estimation approach with Google Earth Engine, *ISPRS J. Photogramm.*
132 *Remote Sens.*, 194, 1-20, doi: 10.1016/j.isprsjprs.2022.10.001, 2022.

133

134 Pinty, B., Andredakis, I., Clerici, M., Kaminski, T., Taberner, M., Verstraete, M. M., Gobron, N.,
135 Plummer, S., and Widlowski, J.-L.: Exploiting the MODIS albedos with the Two-stream Inversion
136 Package (JRC-TIP): 1. Effective leaf area index, vegetation, and soil properties, *J. Geophys. Res.*,
137 116, D09105, doi: 10.1029/2010JD015372, 2011.

138

139 Strobl, C., Boulesteix, A. L., Kneib, T., Augustin, T., and Zeileis, A.: Conditional variable
140 importance for Random Forests, *BMC Bioinformatics*, 9, 307, doi: 10.1186/1471-2105-9-307, 2008.